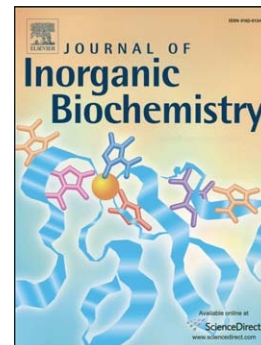


Accepted Manuscript

Synthesis, characterization, X-ray crystal structure, DFT calculation and antibacterial activities of new vanadium(IV, V) complexes containing chelidamic acid and novel thiourea derivatives

Javad Farzanfar, Khaled Ghasemi, Ali Reza Rezvani, Hojat Samareh Delarami, Ali Ebrahimi, Hona Hosseinpour, Amir Eskandari, Hadi Amiri Rudbari, Giuseppe Bruno



PII: S0162-0134(15)00050-1
DOI: doi: [10.1016/j.jinorgbio.2015.02.007](https://doi.org/10.1016/j.jinorgbio.2015.02.007)
Reference: JIB 9668

To appear in: *Journal of Inorganic Biochemistry*

Received date: 1 November 2014
Revised date: 13 February 2015
Accepted date: 13 February 2015

Please cite this article as: Javad Farzanfar, Khaled Ghasemi, Ali Reza Rezvani, Hojat Samareh Delarami, Ali Ebrahimi, Hona Hosseinpour, Amir Eskandari, Hadi Amiri Rudbari, Giuseppe Bruno, Synthesis, characterization, X-ray crystal structure, DFT calculation and antibacterial activities of new vanadium(IV, V) complexes containing chelidamic acid and novel thiourea derivatives, *Journal of Inorganic Biochemistry* (2015), doi: [10.1016/j.jinorgbio.2015.02.007](https://doi.org/10.1016/j.jinorgbio.2015.02.007)

This is a PDF file of an unedited manuscript that has been accepted for publication. As a service to our customers we are providing this early version of the manuscript. The manuscript will undergo copyediting, typesetting, and review of the resulting proof before it is published in its final form. Please note that during the production process errors may be discovered which could affect the content, and all legal disclaimers that apply to the journal pertain.

**Synthesis, characterization, X-ray crystal structure, DFT calculation and
antibacterial activities of new vanadium(IV, V) complexes containing
chelidamic acid and novel thiourea derivatives**

**Javad Farzanfar,^a Khaled Ghasemi,^a Ali Reza Rezvani,^{a,*} Hojat Samareh Delarami,^a Ali
Ebrahimi,^a Hona Hosseinpoor,^a Amir Eskandari,^a Hadi Amiri Rudbari,^b Giuseppe Bruno^c**

^aDepartment of Chemistry, University of Sistan and Baluchestan, Zahedan 98135-674, Iran

^bFaculty of Chemistry, University of Isfahan, Isfahan 81746-73441, Iran

^cUniversita degli Studi di Messina, dip. Scienze Chimiche. Viale Ferdinando S. d'Alcontres, 98166 Messina, Italy

* - Corresponding author Tel: +98 54 33447010; Fax: +98 54 33443388, E-mail address: Ali@hamoon.usb.ac.ir,
javadfr@pgs.usb.ac.ir;

Abstract

Three new thiourea ligands derived from the condensation of aroyl- and aryl-isothiocyanate derivatives with 2,6-diaminopyridine, named 1,1'-(pyridine-2,6-diyl)bis(3-(benzoyl)thiourea) (L1), 1,1'-(pyridine-2,6-diyl)bis(3-(2-chlorobenzoyl)thiourea) (L2) and 1,1'-(pyridine-2,6-diyl)bis(3-(4-chlorophenyl)thiourea) (L3), their oxido-vanadium(IV) complexes, namely $[\text{VO}(\text{L1}')(\text{H}_2\text{O})]$ (C1), $[\text{VO}(\text{L2}')(\text{H}_2\text{O})]$ (C2) and $[\text{VO}(\text{L3}')(\text{H}_2\text{O})]$ (C3), and also, dioxo-vanadium(V) complex containing 4-hydroxy-2,6-pyridine dicarboxylic acid (chelidamic acid, $\text{H}_2\text{dipic-OH}$) and metformin (N,N-dimethylbiguanide, Met), named $[\text{H}_2\text{Met}][\text{VO}_2(\text{dipic-OH})_2 \cdot \text{H}_2\text{O}]$ (C4), were synthesized and characterized by elemental analysis, FTIR and ^1H NMR and UV-visible spectroscopies. Proposed structures for free thiourea ligands and their vanadium complexes were corroborated by applying geometry optimization and conformational analysis. Solid state structure of complex $[\text{H}_2\text{Met}][\text{VO}_2(\text{dipic-OH})_2 \cdot \text{H}_2\text{O}]$ (triclinic, $P\bar{1}$) was fully determined by single crystal X-ray diffraction analysis. In this complex, metformin is double protonated and acted as counter ion. The antibacterial properties of these compounds were investigated in vitro against standard Gram-positive and Gram-negative bacterial strains. The experiments showed that vanadium(IV) complexes had the superior antibacterial activities than novel thiourea derivatives and vanadium(V) complex against all Gram-positive and Gram-negative bacterial strains.

Keywords: Thiourea; 4-hydroxy-2,6-pyridine dicarboxylic acid; N,N-dimethylbiguanide; Oxo-vanadium(IV, V) complex; Antibacterial activity

1. Introduction

In recent years, many research efforts are directed to the development of effective antimicrobial agents caused by the variety of drug-resistant strains and inhibition of the growth of them [1-5]. On the basis of the pharmacological studies of the compounds containing carbonyl and thiocarbonyl groups such as urea, thiourea and their related analogues, it is proposed that the thiourea derivatives and their transition metal complexes represent a wide diversity of biological functions including antibacterial [6-16], antifungal [17-21], anti-diabetic [22-24], antitubercular [25], anti-human immunodeficiency virus (anti-HIV) [26-28], anti-Hepatitis C virus (anti-HCV) [29], Antitumor [30-31], antithyroid, anthelmintic, rodenticidal, insecticidal, herbicidal, and plant-growth regulator properties [32-34]. In many investigations, coordination of thiourea derivatives as potential donor ligands to a range of metal ions have led to increment in the biological activity of these compounds, hence showing that complexation can be a novel approach for the reduction of dose [35]. Vanadium is present in trace amounts as physiologically essential element with wonderful biological properties. There are suggestions that vanadium plays important roles in cells such as regulation of phosphoryl transfer enzymes and cell's redox potential [36]. Pharmacologically, vanadium compounds with oxidation states +4 (IV) and +5 (V) have demonstrated anti-diabetic and anti-carcinogenic effects in humans [37]. Considering the biological properties of vanadium and the antimicrobial activities of thiourea derivatives, it can be concluded that the combination of them can lead to the generation of novel improved antimicrobial agents. In spite of extensive investigations on insulin-enhancing properties and anti-diabetic effects of vanadium compounds, a few researchers have studied antimicrobial activity of vanadium complexes, particularly, with thiourea derivatives as ligands [38-42]. Furthermore, 4-hydroxypyridine-2,6-dicarboxylic acid, which obtains from the substitution of

dipicolinic acid (2,6-pyridine dicarboxylic acid) with a hydroxyl group in position 4 and forms the $[\text{VO}_2(\text{dipic-OH})]^-$ complexes with various organic or inorganic counterions, has recently revealed the range of biological functions [43-45]. In view of this, we focused on the synthesis, characterization and antibacterial activity of three novel thiourea derivatives and their oxido-vanadium(IV) complexes. Moreover, we fully investigated a new dioxo-vanadium(V) complex with metformin, which has lately exhibited an appreciable biological activity, as a counterion namely $[\text{H}_2\text{Met}][\text{VO}_2(\text{dipic-OH})]_2\cdot\text{H}_2\text{O}$. Based upon the previous studies, the protonation of the metformin as a relatively strong base leads to activate it in some biological processes [46]. Since appropriate crystals from pure solid thiourea compounds were not available for X-ray measurements, we carried out geometry optimization and conformational analysis to all free ligands and oxido-vanadium(IV) complexes as a supplementary tool to validate the proposed structures. The antibacterial properties of all compounds were screened in vitro against two standard Gram-positive (*Staphylococcus aureus* and *Enterococcus faecalis*) and two standard Gram-negative (*Escherichia coli* and *Pseudomonas aeruginosa*) bacterial strains.

2. Experimental

2.1. Materials and instrumentation

All starting reagents and solvents were purchased from Sigma-Aldrich and Merck and used as received. Elemental analyses were performed on a Leco, CHNS-932 elemental analyzer. Fourier transform infrared spectra were recorded on a FT-IR JASCO 680-PLUS spectrometer as KBr pellets in the $4000\text{--}400\text{ cm}^{-1}$ spectral range. Proton NMR spectra at room temperature were obtained on a Bruker 400 spectrometer. Electronic spectra (UV-visible (UV-Vis)) were recorded on a UV-JASCO-570 spectrometer using 10 mm pass length quartz cells at room temperature.

2.2. Synthesis

2.2.1. Synthesis of thiourea ligands and their oxido-vanadium(IV) complexes

The ligands L1 and L2 were synthesized using a procedure similar to that described in the literature [8, 47] by the reaction of benzoyl chloride (2 mmol) and 2-chlorobenzoyl chloride (2 mmol) separately with NH_4SCN (2 mmol) in acetone to produce benzoyl-isothiocyanate and 2-chlorobenzoyl-isothiocyanate, respectively, followed by condensation of each of them with 2,6-diaminopyridine (1 mmol). The ligand L3 was directly synthesized by condensation of 4-chlorophenyl-isothiocyanate (2 mmol) with 2,6-diaminopyridine (1 mmol). The oxido-vanadium(IV) complexes were also prepared according to the method described in the literature [48] by the reaction of aqueous solutions (10 ml) of the ammonium metavanadate ($(\text{NH}_4)\text{VO}_3$, 1 mmol) separately with an ethanol solution (10 ml) of each of the ligands (1 mmol) in the presence of triethyl amine. The reaction mixtures were refluxed for 48 h and then the complexes were isolated as the solids. All the resulting solid products (ligands and complexes) were soluble in acetone, ethanol, dichloromethane, DMSO and N,N-dimethylformamide (DMF) and were re-crystallized from an ethanol-dichloromethane mixture (1:2).

L1: Light yellow, m.p.: 156 °C. Anal. Calc. For $\text{C}_{21}\text{H}_{17}\text{N}_5\text{O}_2\text{S}_2$ (%; FW: 435.520 $\text{g}\cdot\text{mol}^{-1}$): C, 57.91; H, 3.93; N, 16.08; S, 14.72; Found: C, 57.83; H, 3.99; N, 16.05; S, 14.78. FTIR (KBr, cm^{-1}): 3330.7, 3107.5, 3032.8, 1667.6, 1599.7, 1580.0, 1552.4, 1537.9, 1531.6, 1515.2, 1489.0, 1451.0, 1399.3, 1325.4, 1319.4, 1239.6, 1152.6, 1100.5, 1072.6, 1021.9, 1000.7, 837.8, 796.4, 772.5, 734.8, 710.9, 687.9, 671.9, 661.8, 648.6, 606.7, 547.8, 476.7, 456.0, 412.9. ^1H NMR (DMSO- d_6 , ppm): 13.21 (br s, 2H, NH), 11.72 (br s, 2H, NH), 7.95-8.84 (m, 10H, phenyl protons), 7.08-7.63 (m, 3H, pyridyl protons). UV-Vis (DMSO, nm): 262, 274, 326.

L2: Light yellow, m.p.: 148 °C. Anal. Calc. For $C_{21}H_{15}Cl_2N_5O_2S_2$ (%; FW: 504.404 $g \cdot mol^{-1}$): C, 50.01; H, 3.00; N, 13.88; S, 12.71; Found: C, 50.08; H, 2.97; N, 13.91; S, 12.75. FTIR (KBr, cm^{-1}): 3390.1, 3221.1, 3180.1, 3111.7, 3046.6, 1676.4, 1592.1, 1577.3, 1556.6, 1536.4, 1477.3, 1449.1, 1440.1, 1402.1, 1328.4, 1305.8, 1250.8, 1239.9, 1161.7, 1097.5, 1044.8, 1022.2, 844.4, 798.6, 771.6, 745.1, 726.7, 711.5, 692.9, 650.7, 617.9, 570.3, 467.9, 438.8. 1H NMR (DMSO- d_6 , ppm): 12.84 (br s, 2H, NH), 11.15 (br s, 2H, NH), 7.83-8.66 (m, 8H, phenyl protons), 7.18-7.69 (m, 3H, pyridyl protons). UV-Vis (DMSO, nm): 260, 271, 323.

L3: Yellow, m.p.: 153 °C. Anal. Calc. For $C_{19}H_{15}Cl_2N_5S_2$ (%; FW: 448.384 $g \cdot mol^{-1}$): C, 50.90; H, 3.37; N, 15.62; S, 14.30; Found: C, 50.84; H, 3.31; N, 15.71; S, 14.24. FTIR (KBr, cm^{-1}): 3397.8, 3373.7, 3325.7, 3197.9, 3030.3, 1582.9, 1532.3, 1484.2, 1448.1, 1401.2, 1350.9, 1305.2, 1260.0, 1222.9, 1195.9, 1156.6, 1089.3, 1013.4, 824.6, 789.7, 771.1, 717.0, 670.1, 627.8, 613.4, 579.0, 495.4, 442.3. 1H NMR (DMSO- d_6 , ppm): 11.20 (br s, 2H, NH), 10.86 (br s, 2H, NH), 7.71-8.63 (m, 8H, phenyl protons), 7.11-7.59 (m, 3H, pyridyl protons). UV-Vis (DMSO, nm): 260, 274, 332.

C1: Green. Anal. Calc. For $C_{21}H_{17}N_5O_4S_2V$ (%; FW: 518.460 $g \cdot mol^{-1}$): C, 48.65; H, 3.31; N, 13.51; S, 12.37; Found: C, 48.63; H, 3.29; N, 13.55; S, 12.38. FTIR (KBr, cm^{-1}): 3431.7, 3332.9, 3165.1, 3107.6, 3032.3, 1667.1, 1603.2, 1579.8, 1514.9, 1489.4, 1448.0, 1399.7, 1309.0, 1218.2, 1206.1, 1186.5, 1152.6, 1101.9, 1073.9, 1020.6, 999.7, 981.3, 826.3, 795.5, 734.8, 711.4, 687.6, 671.3, 661.5, 648.7, 631.4, 606.9, 547.9, 525.4, 479.2, 411.7. UV-Vis (DMSO, nm): 268, 320, 576, 867.

C2: Dark green. Anal. Calc. For $C_{21}H_{15}Cl_2N_5O_4S_2V$ (%; FW: 587.343 $g \cdot mol^{-1}$): C, 42.94; H, 2.57; N, 11.92; S, 10.92; Found: C, 42.88; H, 2.51; N, 12.96; S, 10.96. FTIR (KBr, cm^{-1}): 3471.8, 3337.8, 3219.3, 3178.4, 3111.2, 3043.9, 1676.2, 1592.1, 1577.6, 1556.5, 1533.1, 1477.5,

1448.8, 1402.5, 1305.4, 1221.5, 1161.2, 1097.2, 1044.4, 1021.6, 986.1, 882.7, 844.3, 798.5, 744.9, 726.5, 711.1, 692.6, 650.5, 618.1, 570.3, 528.7, 496.7, 468.1, 438.4. UV-Vis (DMSO, nm): 269, 322, 569, 862.

C3: Dark green. Anal. Calc. For $C_{19}H_{11}Cl_2N_5O_2S_2V$ (%; FW: 527.291 $g \cdot mol^{-1}$): C, 43.28; H, 2.10; N, 13.28; S, 12.16; Found: C, 43.22; H, 2.08; N, 13.32; S, 12.19. FTIR (KBr, cm^{-1}): 3428.3, 3183.4, 3053.2, 1638.6, 1566.3, 1460.1, 1397.1, 1157.9, 985.8, 799.1, 611.0. UV-Vis (DMSO, nm): 267, 324, 560, 859.

2.2.2. Synthesis of dioxo-vanadium(V) complex with chelidamic acid and metformin hydrochloride

4-Hydroxypyridine-2,6-dicarboxylic acid (1.0 mmol) and NaOH (2.0 mmol) were dissolved in the mixture of ethanol/water (20 ml) and dropwise added, under continuous stirring, to an aqueous solution (10 ml) of $VOSO_4$ (1.0 mmol). Afterward metformin hydrochloride (0.50 mmol) was added to the resulting mixture and was refluxed for 18 h until the light green solution obtained. After 6 days, green crystals suitable for X-ray structural analysis from the title dioxo-vanadium(V) complex, C4, were obtained.

C4: pale green, Anal. Calc. For $C_{18}H_{21}N_7O_{15}V_2$ (%; FW: 677.283 $g \cdot mol^{-1}$): C, 31.92; H, 3.13; N, 14.48; Found: C, 31.53; H, 3.07; N, 14.55. FTIR (KBr, cm^{-1}): 3341, 3163, 2749, 1681, 1609, 1572, 1463, 1376, 1290, 1126, 1056, 948, 884, 803, 756, 639, 576, 453. 1H NMR (DMSO- d_6 , ppm): 8.30 (s, dipic- OH^{2-}), 7.61 (s, dipic- OH^{2-}), 7.35 (s, dipic- OH^{2-}), 3.00 (s, 6H, H_2Met). UV-Vis (DMSO, nm): 220, 285.

2.3. Theoretical calculations

To gain an accurate understanding of the molecular structures of thiourea derivatives and their oxido-vanadium(IV) complexes, geometry optimization and conformational analysis performed

in the gas phase with the Gaussian 09 suite of programs and the Beck's three-parameter hybrid method B3LYP with the 6-31G(d,p) basis set. Vibrational frequency analyses were also performed at the same level to ensure the structures are local minima. The natural bond orbital (NBO) method on the wave functions was obtained at the same level of theory by NBO 3.1 program [49-55].

2.4. X-ray crystal structure determination dioxo-vanadium(V) complex C4

The crystal structure of $[\text{H}_2\text{Met}][\text{VO}_2(\text{dipic-OH})_2\cdot\text{H}_2\text{O}]$ was obtained by the single-crystal X-ray diffraction technique. Data for the dioxo-vanadium(V) complex C4 were collected on a Bruker APEX II area-detector diffractometer using graphite monochromated Mo $K\alpha$ radiation, $\lambda = 0.71073 \text{ \AA}$ at 298(2) K. Data was analyzed with APEX2 software, reduced using SAINT program and the empirical absorption corrections were applied using the SADABS program [56]. The structure was solved by direct methods and refined using the least-squares method in SHELXTL software package [57]. All non-hydrogen atoms were refined anisotropically. Outlier reflections were omitted during the final refinement. Materials for publications were prepared with SHELXTL [58], PLATON [58], WinGX [59] and Mercury [60]. Details of the X-ray data collection are reported in Table 1.

2.5. Antibacterial assay

The antibacterial test was done in vitro against two Gram-negative standard strains of bacteria (*Escherichia coli*; *E. coli* ATCC 25922 and *Pseudomonas aeruginosa*; *P. aeruginosa* ATCC 27853) and two Gram-positive standard strains of bacteria (*Staphylococcus aureus*; *S. aureus* ATCC 25923 and *Enterococcus faecalis*; *E. faecalis* ATCC 11700).

2.5.1. Determination of minimum inhibitory concentration

Minimum inhibitory concentrations for all synthesized thioureas and vanadium(IV, V) complexes were investigated against all above-named standard bacterial strains by the broth macrodilution assay in sterile test tubes [61]. The Muller Hinton Broth (MLB) medium was used. Since DMSO has no effect on the microorganisms, DMSO was used as solvent for preparation of stock solutions and further dilutions were done with distilled water. The concentrations of assayed compounds were 1024, 512, 256, 128, 64, 32, 16, 8, 4, 2 and 1 $\mu\text{g/ml}$. DMSO was utilized as negative control. In nutrient broth medium 24 h fresh bacterial culture was prepared. In order to compare the turbidity of bacterial culture, McFarland Standard 0.5 solution was used as turbidity standard. All the inoculated tubes were incubated at 36 °C and results were assessed after 18 h for bacteria. The minimum inhibitory concentration (MIC) was defined as the lowest concentration of the compounds that prevents the visible growth of bacteria after incubation for 18 h, at 36 °C.

2.5.2. Determination of inhibition zone

The inhibition zones of the synthesized compounds were determined in vitro against all aforesaid standard bacterial strains by the disk diffusion method. Sterilized paper disks (diameter = 6 mm) were immersed in DMSO solution of tested compounds in the concentration equivalent to most obtained MIC for 5 min. Then, they were taken out and attached to the surface of Muller Hinton Agar (MHA) plates, which were inoculated with a loop (0.01 cm^3) of the adequate inoculum of the bacteria ($10^6 \text{ CFUs cm}^{-3}$). DMSO was used as a negative control while Amikacin (AMK-30 μg) and Gentamycin (GEN-10 μg) were used as positive controls for Gram positive antibacterial activity and Gram negative antibacterial activity, respectively. All plates were incubated for 24 h at 36 °C and the resulting diameter of each inhibition zone showing no bacterial growth was measured.

3. Results and Discussion

3.1. Characterization of thiourea ligands and their oxido-vanadium(IV) complexes

3.1.1. Infrared spectroscopy

The solid state properties of three new thiourea ligands and their oxido-vanadium(IV) complexes were investigated by infrared spectroscopy. The infrared spectra of these samples exhibit all the expected frequency regions of the $\nu(\text{N-H})$, $\nu(\text{C=S})$, $\nu(\text{C=O})$ and $\nu(\text{C-N})$. The thiourea derivatives can display thione-thiol tautomerism. In the IR spectra of the ligands, the $\nu(\text{S-H})$ band at around $2500\text{-}2600\text{ cm}^{-1}$ is absent and, vice versa, multiple absorption bands related to the asymmetric and symmetric stretching vibrations of the (N-H) groups in the range of $3100\text{-}3400\text{ cm}^{-1}$ are present, consequently, exhibiting formation of the thione tautomer in the solid state of thiourea derivatives. The absorption band at about 3030 cm^{-1} is assigned to $\nu(\text{Ph-H})$ stretching mode. The characteristic IR bands associated with the stretching vibrations of thionyl (C=S) groups of the free thiourea ligands are appeared in the region of $1325\text{-}1351$, $1239\text{-}1260$ and $824\text{-}844\text{ cm}^{-1}$. The multiple high or medium intensity absorption bands in the range of $1000\text{-}1200\text{ cm}^{-1}$ are attributed to the $\nu(\text{C-N})$ stretching vibrations. The $\nu(\text{C=C}) + \nu(\text{C=N})$ vibration frequencies of the pyridine ring found at around $1515\text{-}1600\text{ cm}^{-1}$. The ring wagging vibrations of the pyridine group are observed in the range of $670\text{-}692$ and $789\text{-}798\text{ cm}^{-1}$. The absorption band at around 610 cm^{-1} is from the in-plane ring deformation of the pyridine ring. For two thiourea ligands L1 and L2, the sharp absorption band at about 1670 cm^{-1} is responsible for the stretching vibration of carbonyl (C=O) group. Besides, the absorption band observed at around 710 cm^{-1} corresponds to $\nu(\text{C-Cl})$ stretching vibration of phenyl ring in two thiourea ligands L2 and L3 [47-48].

In the suggested structures of the complexes C1 and C2 (Figures 1 and 2), two thiourea ligands L1 and L2, respectively, behave as binegative tridentate chelating agents coordinating through the nitrogen of the pyridyl group and two CS groups in the thiol form to vanadyl ($[\text{VO}]^{2+}$) ion. The environment around the vanadium atom is penta-coordinate. In the IR spectra of these complexes, two $\nu(\text{C}=\text{S})$ bands of free thiourea ligands at around 1325 and 1239 cm^{-1} underwent a shift into lower frequencies at about 1305 and 1220 cm^{-1} and the $\nu(\text{C}=\text{S})$ band of free thiourea ligands at around 840 cm^{-1} weakened upon complexation. These observations suggest the participation of the C=S groups in the coordination, which are in acceptable agreement with the proposed structures of the complexes C1 and C2 [7].

The synthesis of complex C3 starts with the reaction of the sulfur atoms in thionyl (C=S) groups with carbon atoms (C17 and C28) in the phenyl rings of the free thiourea ligand L3, which eliminates four hydrogen atoms and forms two new five-membered rings. In the suggested structure of the complex C3 (Fig. 3), the oxidized cyclization form of thiourea ligand L3 acts as a binegative tridentate chelating ligand coordinating through the nitrogen atoms of pyridine and thiourea to vanadyl ($[\text{VO}]^{2+}$) ion. Similarly with the complexes C1 and C2, The environment around the vanadium atom of complex C3 is penta-coordinate. In the IR spectrum of this complex, the $\nu(\text{C}=\text{S})$ band of free thiourea ligand L3 at 824 cm^{-1} is absent and the new absorption band observed at 799 cm^{-1} corresponds to $\nu(\text{C}-\text{S})$ stretching vibration upon cyclization [47].

According to the literature, the oxido-vanadium(IV) complexes display the IR band related to the stretching vibration of vanadyl (V=O) group in the region of 995-940 cm^{-1} . This characteristic band for the square pyramidal oxido-vanadium(IV) complexes emerges at higher wave numbers, while for octahedral oxido-vanadium(IV) complexes appears at 960–940 cm^{-1} . For example,

Bakir J.A. Jeragh *et al.* studied three monomeric square pyramidal oxido-vanadium(IV) complexes containing para-substituted phenyl-2-picolyketone. The IR band of vanadyl group for these complexes was observed in the range of 977–993 cm^{-1} [62]. In the IR spectra of present oxido-vanadium(IV) complexes (C1, C2 and C3), the characteristic IR absorption band associated with the stretching vibration of vanadyl (V=O) group is appeared at around 985 cm^{-1} and the broad absorption band at around 3425 cm^{-1} is attributed to the $\nu(\text{H}_2\text{O})$ stretching vibrations of coordinated water molecule. Their wide broadness is representative of an intensive H-bonding [63].

3.1.2. Electronic absorption spectroscopy

DMSO solutions of three new thiourea ligands and their oxido-vanadium(IV) complexes were prepared, and their electronic absorption spectra were recorded in the range of 200-1000 nm. Electronic excitation study of these samples in DMSO solution display several absorption bands in the UV and visible regions. For all thiourea ligands, in the UV region, three intense absorption bands in the range of 260-262, 271-274 and 323-332 nm were assigned to intra-ligand $\pi \rightarrow \pi^*$ and $n \rightarrow \pi^*$ charge transfer transitions from phenyl and pyridine rings of the free thiourea ligands.

According to the literature, the square pyramidal oxido-vanadium(IV) complexes display three characteristic d–d transition bands with low intensities in the visible region. Electronic excitation study of oxido-vanadium(IV) complexes in DMSO solution result in the addition of DMSO trans to the oxygen in the vanadyl moiety. Therefore, the third band in DMSO is mostly absent due to a blue shift for the d–d transitions [64]. For example, Bakir J.A. Jeragh *et al.* observed that their monomeric square pyramidal oxido-vanadium(IV) complexes exhibit two d–d transition bands in the visible region and the third band is absent [62]. For present oxido-vanadium(IV) complexes (C1, C2 and C3), in the UV region, two strong bands at around 268 and 322 nm are related to

intra-ligand charge transfer transitions within the thiourea moiety of the complexes and in the visible region, the weak bands in the range of 560-867 nm are assigned to d-d transitions within the oxido-vanadium(IV) moiety of the complexes [7, 65].

3.1.3. NMR spectroscopy

Proton NMR spectroscopy was recorded in CDCl₃ at room temperature at 400.00 MHz on a Bruker 400 instrument. ¹H NMR spectra of three new thiourea ligands manifested the expected characteristic resonances, multiplicity and integration consistent with the corresponding structures. In the ¹H NMR spectra of the all free thiourea ligands, the characteristic signals for the protons on the pyridyl ring were observed at around δ_{H} 7.08-7.69 ppm, while the characteristic signals for the protons on the phenyl rings were recognized in downfield about δ_{H} 7.71-8.84 ppm. Moreover, the NH resonances notably were downfield from other resonances and as seen, NH signals were observed in the range of δ_{H} 10.86-13.21 ppm as two broad singlet signals in the ¹H NMR spectra.

3.1.4. Theoretical studies

The optimization of the molecular structures of the free thiourea ligands and their oxido-vanadium(IV) complexes were performed at the DFT (Density Functional Theory) level of theory. The most important geometrical parameters of the target compounds are gathered in Tables 2 and 3. The configurations of transition metal complexes with five-coordinate atoms around metal ion can range from regular trigonal-bipyramidal (RTBP) to regular square-based pyramidal (RSBP) coordination. According to N6-V-O25 (145.84° in C1 and 127.52° in C3), N14-V-N27 (158.40° in C3), S13-V-S26 (149.07 ° in C1) angles, configurations of complexes are RSBP and coordination is occurred through the nitrogen of the pyridyl group and two CS groups in the thiol form with vanadyl ([VO]²⁺) ion. As can be seen from Tables 2 and 3, N10-

C12 bond length in C1 and C2 is shorter than that in L1 and L2. Also, C12-S13 and N6-C5 bond lengths in these complexes are longer than those in the corresponding ligands. These results confirm suggested coordination through the nitrogen of the pyridyl group and two CS groups in the thiol form with vanadyl ion. On the other hand, contraction of N10-C12 and C12-N14 bonds with the elongation of N6-C5 and C12-S13 bonds confirm the mentioned coordination in C3 complex.

The frontier molecular orbitals (HOMO and LUMO) of thiourea ligands and their complexes are presented in Fig. 4. In addition, some considerable electronic features such as calculated natural charges of atoms, dipole moments and energies of HOMO and LUMO for all thiourea ligands and complexes are listed in Table 4. As can be seen, in the HOMO molecular orbitals, the higher negative charge density is around sulphur atoms of thiourea ligands, which can increase probability of nucleophilic attack from those to metal ion. It can be found that more negative charge on S13 and simultaneously less negative charges on N10 and N14 have led to nucleophilic attack of the sulfur atoms in thionyl (C=S) groups to carbon atoms (C17 and C28) in the phenyl rings and formation of two new five-membered rings in the free thiourea ligand L3. The higher energy of HOMO and the lower energy of LUMO facilitate the interaction between the donor and acceptor of electron. On the basis of the obtained results from previous antibacterial studies [6], the quantity of difference between LUMO and HOMO energies (ΔE_{L-H}) and the level of the LUMO energies (E_{LUMO}) play important roles in the antibacterial activities of these compounds.

3.2. Characterization of dioxo-vanadium(V) complex with chelidamic acid and metformin hydrochloride

3.2.1. Infrared spectroscopy

The solid state properties of the dioxo-vanadium(V) complex C4 was investigated by infrared spectroscopy. The infrared spectrum of complex C4 shows strong, broad and branched absorption bands at 2749–3500 cm^{-1} because of the O–H stretching vibrations of the crystallization water molecules, aliphatic C–H's of metformin, aromatic C–H's of pyridyl ring and NH_2^+ stretching vibrations of metformin. The strong characteristic absorption bands at 1681 and 1376 cm^{-1} corresponds to the asymmetric and symmetric stretching vibrations of carboxyl groups, respectively. Furthermore, this complex exhibited one strong absorption band at 1056 cm^{-1} , which is attributed to the C–O (hydroxy) vibration of dipic-OH ligand. In the IR spectrum of the dioxo-vanadium(V) complex C4, two characteristic absorption bands associated with the symmetric and asymmetric stretching vibrations of (V=O) group are observed at 948 and 884 cm^{-1} , respectively. This behavior is consistent with previously reported dioxo-vanadium(V) complexes of the dipicolinic acid and derivatives [66-67].

3.2.2. Electronic absorption spectroscopy

DMSO solution of the dioxo-vanadium(V) complex C4 was prepared, and its electronic spectrum was recorded in the range of 200-1000 nm. Electronic excitation study of this sample in DMSO solution shows two absorption bands in the UV region. The absorption bands at 220 and 285 nm were assigned to the intra-ligand $\pi \rightarrow \pi^*$ and $n \rightarrow \pi^*$ charge transfer transitions in the dipic-OH ligand. The band at 220 nm was probably superimposed with the O \rightarrow V charge transfer involving the double bonded oxo group.

3.2.3. NMR spectroscopy

Proton NMR spectrum of the dioxo-vanadium(V) complex C4 confirms the presence of both Met and $(\text{dipic-OH})^{2-}$ fragments in this complex and gives four signals in DMSO-d_6 at δ_{H} 3.00, 7.35, 7.61 and 8.30 ppm. The resonance at δ_{H} 3.00 ppm is assigned to methyl protons of metformin

and the remaining three resonances correspond to aromatic protons of the pyridyl ring in (dipic-OH)²⁻.

3.2.4. Description of the crystal structure of the dioxo-vanadium(V) complex C4

The molecular and crystal structure of dioxo-vanadium(V) complex C4 was fully elucidated by single crystal X-ray diffraction methods. The ORTEP view of the molecular structure of C4 is shown in Fig. 5, together with the atomic labelling scheme. A list of the most important bond distances and angles is reported in Table 5.

The vanadium atom shows a penta-coordinate environment, achieved by two oxo ligands and by the tridentate (dipic-OH)²⁻ moiety. The configurations of transition metal complexes with five-coordinate atoms can range from regular trigonal-bipyramidal (RTBP, D_{3h}) to regular square-based pyramidal (RSBP, C_{4v}) coordination. In order to assign the corrected geometrical environment as trigonal-bipyramidal or squared pyramidal to the vanadium atom, the τ parameter defined in [68] can be considered. However, the numerical value of 0.32 in compound C4 didn't allow assigning unambiguously the corrected geometrical coordination.

The (dipic-OH)²⁻ ligands are planar and the mean plane of the ligand bisects the dioxo-vanadium V=O double bonds whose lengths are range from 1.603(3) to 1.617(3) Å (average 1.61 Å). The V-N_{py} and V-O_{carb} bond distances are V1-N6 2.072(3) Å, V1-O1 1.977(3) Å, V1-O3 1.990(2) Å and V2-N7 2.076(3) Å, V2-O12 1.606(3) Å, V2-O13 1.603(3) Å (Table 5).

The asymmetric unit of compound C4 is constituted by two molecular anion [VO₂(dipic-OH)]⁻, a molecular cation [H₂Met]²⁺ and a water molecule. The cation lies on a symmetry center. The crystal packing is build up by several mediums to strong hydrogen bond interactions (Table 6 and Fig. 6). In particular the nitrogen atom of the cation [H₂Met]²⁺ is involved in two hydrogen bonds with two carboxylic oxygen atom of the anion [VO₂(dipic-OH)]⁻ [N(1)⋯O(2) 2.933(4) Å,

N(1)–H(1B)···O(2) 148(3)° and N(1)···O(11) 2.869(4) Å, N(1)–H(1A)···O(11) 162(4)°]. Moreover, the water molecule is involved in three hydrogen bonds with two oxo and a carboxylic oxygen atoms, [O15···O5 3.028(4) Å, O(15)–H(15B)···O(5) 148(6)°, O15···O6 3.026(4) Å, N(15)–H(15B)···O(6) 139(6)° and O15···O10 2.554(1) Å, O(15)–H(15A)···O(10) 157(4)°].

3.3. Antibacterial activities

All studied compounds were screened for antibacterial activity in terms of the minimum inhibitory concentration (MIC) by the broth macrodilution procedure and the zone of inhibition by the disk diffusion method against different types of bacterial strains. The experiments were repeated three parallel times. The values of minimum inhibitory concentrations and inhibition zones of the all compounds are reported as means of at least three determinations and are represented in Table 7. As is apparent from the table all compounds revealed relatively good inhibitory activities against the all bacterial strains, compared to standard drugs as positive controls used for comparison purposes. It can also be drawn from the table that relative to negative control DMSO, all compounds have stronger antibacterial activities. The antibacterial activities of oxo-vanadium(IV, V) complexes are relatively higher than those of three new thiourea ligands, hence verifying that coordination with vanadium ion leads to increment in the biological activity of these thiourea derivatives. This increment in the antibacterial activity may be because of the formation of the chelate, which decreases the polarity of the compound and thereby increases the lipophilic properties. The improved lipophilic characteristics facilitate the interaction of these complexes with cell components and processes. Moreover, the antibacterial activities of the oxido-vanadium(IV) complexes are the highest against all types of bacterial strains. All compounds inhibited the growth of bacteria with MIC values ranging between 64 and

1024 $\mu\text{g/ml}$. On precise examination of the theoretical results, it can be found that antibacterial activities have some relationship with the LUMO energies and the difference between LUMO and HOMO energies (Figures 7 and 8). We find that the thickness of inhibition zones for above-named standard bacterial strains is linear with these features in some samples. For example, the differences between the LUMO and HOMO energies in L2, L3, C1, C2, C3 and C4 compounds are linear with the thickness of inhibition zones for *P. aeruginosa*, namely, the lower difference between LUMO and HOMO energies leads to higher antibacterial activity. The linear equation is $y = -101.2x + 33.61$, $R^2 = 0.872$. These relations may attribute to the more appropriate interaction of these complexes with cell components and processes because of the accessibility of the suitable orbitals. Figures 7 and 8 demonstrate more instances of these connections.

4. Conclusions

Present research investigated the synthesis, characterization, crystal structure, theoretical calculation and antibacterial properties of three thiourea ligands, their oxido-vanadium(IV) complexes and dioxo-vanadium(V) complex containing chelidamic acid and metformin. From the chemical structures of the resulting oxido-vanadium(IV) complexes, it can be concluded that the configurations of oxido-vanadium(IV) complexes around the vanadium atom are square-based pyramidal coordination. Theoretical calculations show that the antibacterial activities of thiourea ligands and their oxido-vanadium(IV) complexes have some relation with the LUMO energy and the difference between LUMO and HOMO energies. The results of antibacterial experiments show that all the synthesized compounds have good ability to inhibit growth of the bacteria. Considering the antibacterial activities of these compounds, we are currently working

on the vanadium complexes with other thiourea ligands for the investigation of their biological properties.

5. Abbreviations

L1	1,1'-(pyridine-2,6-diyl)bis(3-(benzoyl)thiourea)
L2	1,1'-(pyridine-2,6-diyl)bis(3-(2-chlorobenzoyl)thiourea)
L3	1,1'-(pyridine-2,6-diyl)bis(3-(4-chlorophenyl)thiourea)
C1	[VO(L1')(H ₂ O)]
C2	[VO(L2')(H ₂ O)]
C3	[VO(L3')(H ₂ O)]
C4	[H ₂ Met][VO ₂ (dipic-OH)] ₂ ·H ₂ O
HIV	Human immunodeficiency virus
HCV	Hepatitis C virus
H ₂ dipic-OH	4-Hydroxy-2,6-pyridine dicarboxylic acid
Met	N,N-Dimethylbiguanide
DMF	N,N-dimethylformamide
DFT	Density functional theory
m.p.	Melting point
MLB	Muller Hinton Broth
MHA	Muller Hinton Agar
MIC	Minimum inhibitory concentration
AMK	Amikacin
GEN	Gentamycin

RTBP	Regular trigonal-bipyramidal
RSBP	Regular square-based pyramidal
HOMO	Highest Occupied Molecular Orbital
LUMO	Lowest Unoccupied Molecular Orbital
FW	Formula weight

Acknowledgement

The authors are grateful to the University of Sistan and Baluchestan (USB) for financial support.

Appendix A. Supplementary materials

Full crystallographic data for the structural analysis have been deposited with the Cambridge Crystallographic Data Center, CCDC No. 1031492. This data can be obtained free of charge via www.ccdc.cam.ac.uk or from Cambridge Crystallographic Data Center, 12 Union Road, Cambridge, CB2, 1EZ, UK (fax: +44 (0)1223 336033 or email: deposit@ccdc.cam.ac.uk).

References

- [1] A. Khalaj, M. Nakhjiri, A.S. Negahbani, M. Samadizadeh, L. Firoozpour, S. Rajabalian, N. Samadi, M.A. Faramarzi, N. Adibpour, A. Shafiee, A. Foroumadi, *Eur. J. Med. Chem.* 46 (2011) 65–70.
- [2] M.S. Karthikeyan, D.J. Prasad, B. Poojary, K.S. Bhat, B.S. Holla, N.S. Kumari, *Bioorg. Med. Chem.* 14 (2006) 7482–7489.
- [3] X.S. Cui, C. Jing, K.Y. Chai, J.S. Lee, Z.S. Quan, *Med. Chem. Res.* 18 (2009) 49–58.

- [4] J. Chen, X.Y. Sun, K.Y. Chai, J.S. Lee, M.S. Song, Z.S. Quan, *Bioorg. Med. Chem.* 15 (2007) 6775–6781.
- [5] X.J. Chen, F. Niyonsaba, H. Ushio, D. Okuda, I. Nagaoka, S. Ikeda, K. Okumura, H. Ogawa, *J. Dermatol. Sci.* 40 (2005) 123–132.
- [6] W. Yang, H. Liu, M. Li, F. Wang, W. Zhou, J. Fan, *J. Inorg. Biochem.* 116 (2012) 97–105.
- [7] U. El-Ayaan, *J. Mol. Struct.* 998 (2011) 11–19.
- [8] H. Arslan, N. Duran, G. Borekci, C.K. Ozer, C. Akbay, *Molecules* 14 (2009) 519–527.
- [9] Z. Zhong, R. Xing, S. Liu, L. Wang, S. Caia, P. Li, *Carbohydr. Res.* 343 (2008) 566–570.
- [10] M.Kh. Rauf, I. Din, A. Badshah, M. Gielen, M. Ebihara, D.D. Vos, S. Ahmed, *J. Inorg. Biochem.* 103 (2009) 1135–1144.
- [11] S.A. Khan, N. Singh, K. Saleem, *Eur. J. Med. Chem.* 43 (2008) 2272–2277.
- [12] G. Binzet, H. Arslan, U. Flörke, N. Külçü, N. Duran, *J. Coord. Chem.* 59 (2006) 1395–1406.
- [13] S. Cunha, F.C. Macedo Jr., G.A.N. Costa, M.T. Rodrigues Jr., R.B.V. Verde, L.C.D.S. Neta, I. Vencato, C. Lariucci, F.P. Sa, *Monatsh. Chem.* 138 (2007) 511–516.
- [14] A.A. Isab, S. Nawaz, M. Saleem, M. Altaf, M. Monim-ul-Mehboob, S. Ahmad, H.S. Evans, *Polyhedron* 29 (2010) 1251–1256.
- [15] A. Saeed, U. Shaheen, A. Hameed, S.Z. Haider Naqvi, *J. Fluorine Chem.* 130 (2009) 1028–1034.
- [16] G.S. Kurt, F. Sevgi, B. Mercimek, *Chem. Pap.* 63 (2009) 548–553.
- [17] E. Rodríguez-Fernández, E. García, M.R. Hermosa, A. Jiménez-Sánchez, M.M. Sánchez, E. Monte, J.J. Criado, *J. Inorg. Biochem.* 75 (1999) 181–188.
- [18] Z. Weiqun, Y. Wen, X. Liqun, C. Xianchen, *J. Inorg. Biochem.* 99 (2005) 1314–1319.

- [19] R.D. Campo, J.J. Criado, R. Gheorghe, F.J. Gonzalez, M.R. Hermosa, F. Sanz, J.L. Manzano, E. Monte, E. Rodriguez-Fernandez, *J. Inorg. Biochem.* 98 (2004) 1307–1314.
- [20] F. Bilek, T. Krizova, M. Lehocky, *Colloids Surf B Biointerfaces* 88 (2011) 440–447.
- [21] R.D. Campo, J.J. Criado, E. Garcia, M.R. Hermosa, A. Jimenez-Sanchez, J.L. Manzano, E. Monte, E. Rodriguez-Fernandez, F. Sanz, *J. Inorg. Biochem.* 89 (2002) 74–82.
- [22] H. Pluempfe, W. Pulls, *Chem. Abstr.* 74 (1971) 1251154n.
- [23] H.M. Faidallah, K.A. Khan, A.M. Asiri, *J. Fluorine Chem.* 132 (2011) 131–137.
- [24] H.M. Faidallah, K.A. Khan, A.M. Asiri, *J. Fluorine Chem.* 132 (2011) 870–877.
- [25] S. Karakus, S. Rollas, *Il Farmaco* 57 (2002) 577–581.
- [26] S.B. Tsogoeva, M.J. Hateley, D.A. Yalalov, K. Meindl, C. Weckbecker, K. Huthmacher, *Bioorg. Med. Chem.* 13 (2005) 5680–5685.
- [27] O.J. DCruz, Y. Dong, F.M. Uckun, *Biochem. Biophys. Res. Commun.* 302 (2003) 253–264.
- [28] T.K. Venkatachalam, E.A. Sudbeck, F.M. Uckun, *Tetrahedron Lett.* 42 (2001) 6629–6632.
- [29] I.J. Kang, L.W. Wang, C.C. Lee, Y.C. Lee, Y.S. Chao, T.A. Hsu, J.H. Chern, *Bioorg. Med. Chem. Lett.* 19 (2009) 1950–1955.
- [30] W. Hermindez, E. Spodine, L. Beyer, U. Schrtider, R. Richter, J. Ferreira, M. Pavani, *Bioinorg. Chem. Appl.* 3 (2005) 3–4.
- [31] W. Hermindez, E. Spodine, J.C. Mufioz, L. Beyer, U. Schrtider, R. Richter, J. Ferreira, M. Pavani, *Bioinorg. Chem. Appl.* 1 (2003) 3–4.
- [32] E. Rodríguez-Fernández, J.L. Manzano, J.J. Benito, R. Hermosa, E. Monte, J.J. Criado, *J. Inorg. Biochem.* 99 (2005) 1558–1572.
- [33] M.K. Rauf, I.A. Badshah, M. Gielen, M. Ebihara, D. de Vos, S. Ahmed, *J. Inorg. Biochem.* 103 (2009) 1135–1144.

- [34] H.J. Zhang, X. Qin, K. Liu, D.D. Zhu, X.M. Wang, H.L. Zhu, *Bioorg. Med. Chem.* 19 (2011) 5708–5715.
- [35] I.C. Mendes, M.A. Soares, R.G. dos Santos, C. Pinheiro, H. Beraldo, *Eur. J. Med. Chem.* 44 (2009) 1870–1877.
- [36] F.H. Nielsen, *FASEB J.* 5 (1991) 2661–2667.
- [37] M. Anke, H. Illing-Gunther, U. Schafer, *Biomed. Res. Trace Elem.* 16 (2005) 208–214.
- [38] G. Müller, H. Benkhai, R. Matthes, B. Finke, W. Friedrichs, N. Geist, W. Langel, A. Kramer, *Biomaterials* 35 (2014) 5261–5277.
- [39] I.O. Adriazola, A.E. doAmaral, J.C. Amorim, B.L. Correia, C.L.O. Petkowicz, A.L.R. Mercê, G.R. Noleto, *J. Inorg. Biochem.* 132 (2014) 45–51.
- [40] Z.H. Chohan, S.H. Sumrra, M.H. Youssoufi, T.B. Hadda, *Eur. J. Med. Chem.* 45 (2010) 2739–2747.
- [41] T. Rosu, E. Pahontu, M. Reka-Stefana, D.C. Ilies, R. Georgescu, S. Shova, A. Gulea, *Polyhedron* 31 (2012) 352–360.
- [42] S.H. Sumrra, Z.H. Chohan, *Spectrochim. Acta, Part A* 98 (2012) 53–61.
- [43] D.C. Crans, M. Mahroof-Tahir, M.D. Johnson, P.C. Wilkins, L. Yang, K. Robbins, A. Johnson, J.A. Alfano, M.E. Godzala, L.T. Austin, G.R. Willsky, *Inorg. Chim. Acta* 356 (2003) 365–378.
- [44] L. Yang, A. la Cour, O.P. Anderson, D.C. Crans, *Inorg. Chem.* 41 (2002) 6322–6331.
- [45] T.G. Porter and D.L. Martin, *Biochem. Pharmacol.* 34 (1985) 4145–4150.
- [46] I. Sánchez-Lombardo, E. Sánchez-Lara, A. Pérez-Benítez, Á. Mendoza, S. Bernès, E. González-Vergara, *Eur. J. Inorg. Chem.* (2014) 4581–4588.
- [47] G. Li, D.J. Che, Z.F. Li, Y. Zhu, D.P. Zou, *New J. Chem.* 26 (2002) 1629–1633.

- [48] C.K. Ozer, H. Arslan, D. VanDerveer, G. Binzet, J. Coord. Chem. 62 (2009) 266-276.
- [49] A.D. Becke, Density-Functional Thermochemistry. III. The Role of Exact Exchange. J. Chem. Phys. 98 (1993) 5648–5652.
- [50] C. Lee, W. Yang, R.G. Parr, Development of the Colle-Salvetti Correlation-Energy Formula into a Functional of the Electron Density. Phys. Rev. B 37 (1988) 785–789.
- [51] M.J. Frisch, G.W. Trucks, H.B. Schlegel, G.E. Scuseria, M.A. Robb, J.R. Cheeseman, G. Scalmani, V. Barone, B. Mennucci, G.A. Petersson, H. Nakatsuji, M. Caricato, X. Li, H.P. Hratchian, A.F. Izmaylov, J. Bloino, G. Zheng, J.L. Sonnenberg, M. Hada, M. Ehara, K. Toyota, R. Fukuda, J. Hasegawa, M. Ishida, T. Nakajima, Y. Honda, O. Kitao, H. Nakai, T. Vreven, J.A. Montgomery, J.E. Peralta, F. Ogliaro, M. Bearpark, J.J. Heyd, E. Brothers, K.N. Kudin, V.N. Staroverov, R. Kobayashi, J. Normand, K. Raghavachari, A. Rendell, J.C. Burant, S.S. Iyengar, J. Tomasi, M. Cossi, N. Rega, J.M. Millam, M. Klene, J.E. Knox, J.B. Cross, V. Bakken, C. Adamo, J. Jaramillo, R. Gomperts, R.E. Stratmann, O. Yazyev, A.J. Austin, R. Cammi, C. Pomelli, J.W. Ochterski, R.L. Martin, K. Morokuma, V.G. Zakrzewski, G.A. Voth, P. Salvador, J.J. Dannenberg, S. Dapprich, A.D. Daniels, O. Farkas, J.B. Foresman, J.V. Ortiz, J. Cioslowski, D.J. Fox, Gaussian 09, Revision A.1, Gaussian, Inc., Wallingford CT, 2009.
- [52] E.D. Glendening, A.E. Reed, J.E. Carpenter, F. Weinhold, NBO 3.1; Theoretical Chemistry Institute, University of Wisconsin: Madison, 1990.
- [53] G. Micera and E. Garribba, Int. J. Quantum Chem. 112 (2012) 2486–2498.
- [54] G. Micera, V.L. Pecoraro, E. Garribba, Inorg. Chem. 48 (2009) 5790–5796.
- [55] S. Gorelsky, G. Micera, E. Garribba, Chem. Eur. J. 16 (2010) 8167 – 8180.
- [56] Bruker, SAINT and SMART, Bruker AXS Inc., Madison, Wisconsin, USA, 2009.
- [57] G.M. Sheldrick, Acta Crystallogr., Sect. A 64 (2008) 112–122.

- [58] A.L. Spek, *Acta Crystallogr., Sect. D* 65 (2009) 148–155.
- [59] L.J. Farrugia, *J. Appl. Crystallogr.* 45 (2012) 849–854.
- [60] C.F. Macrae, P.R. Edgington, P. McCabe, E. Pidcock, G.P. Shields, R. Taylor, M. Towler, J.V.D. Streek, *J. Appl. Crystallogr.* 39 (2006) 453–457.
- [61] I. Wiegand, K. Hilpert, R.E.W. Hancock, *Nature Protocols* 3 (2008) 163–175.
- [62] B.J.A. Jeragh and A. El-Dissouky, *Transition Met. Chem.* 29 (2004) 579–585.
- [63] K. Nakamoto, *Infrared and Raman Spectra of Inorganic and Coordination Compounds*. Wiley-Interscience, New York, 1997.
- [64] C.J. Ballhausen and H.B. Gray, *Inorg. Chem.* 1 (1962) 111–122.
- [65] H.Y. Zhao, Y.H. Zhang, Y.H. Xing, Z.P. Li, Y.Z. Cao, M.F. Ge, X.Q. Zeng, S.Y. Niu, *Inorg. Chim. Acta* 362 (2009) 4110–4118.
- [66] B.S. Parajo'n-Costa, O.E. Piro, R. Pis-Diez, E.E. Castellano, A.C. Gonzalez-Baro, *Polyhedron* 25 (2006) 2920–2928.
- [67] D.C. Crans, M. Mahroof-Tahir, M.D. Johnson, P.C. Wilkins, L. Yang, K. Robbins, A. Johnson, J.A. Alfano, M.E. Godzala, L.T. Austin, G.R. Willsky, *Inorg. Chim. Acta* 356 (2003) 365–378.
- [68] A.W. Addison, T.N. Rao, J. Reedijk, J. van Rijn, G.C. Verschoor, *J. Chem. Soc., Dalton Trans.* (1984) 1349.

Figure legends

Fig. 1. The minimum energy structures of the ligand L1 and complex C1.

Fig. 2. The minimum energy structures of the ligand L2 and complex C2.

Fig. 3. The minimum energy structures of the ligand L3 and complex C3.

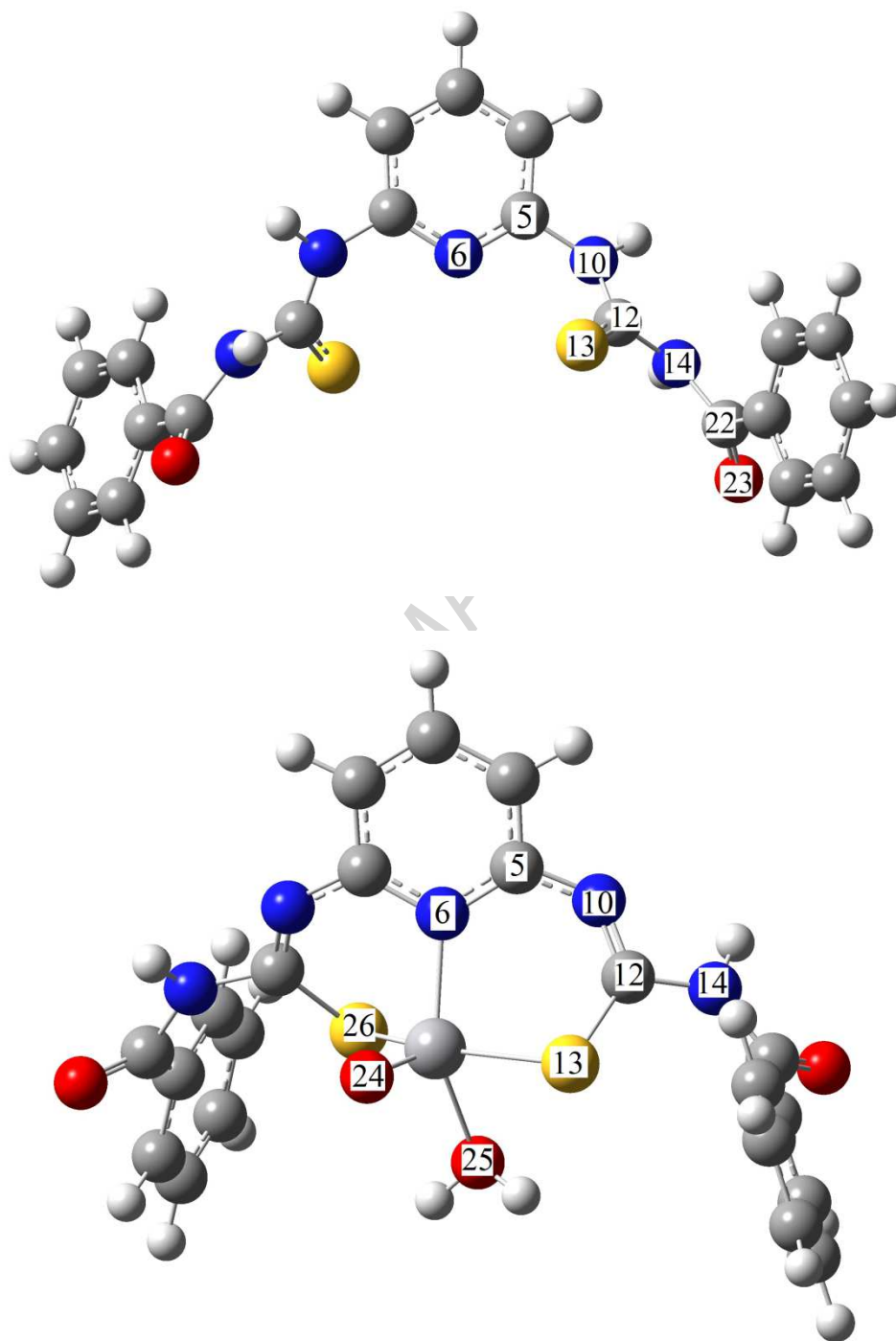
Fig. 4. HOMO and LUMO Molecular orbitals of the thiourea ligands and their complexes.

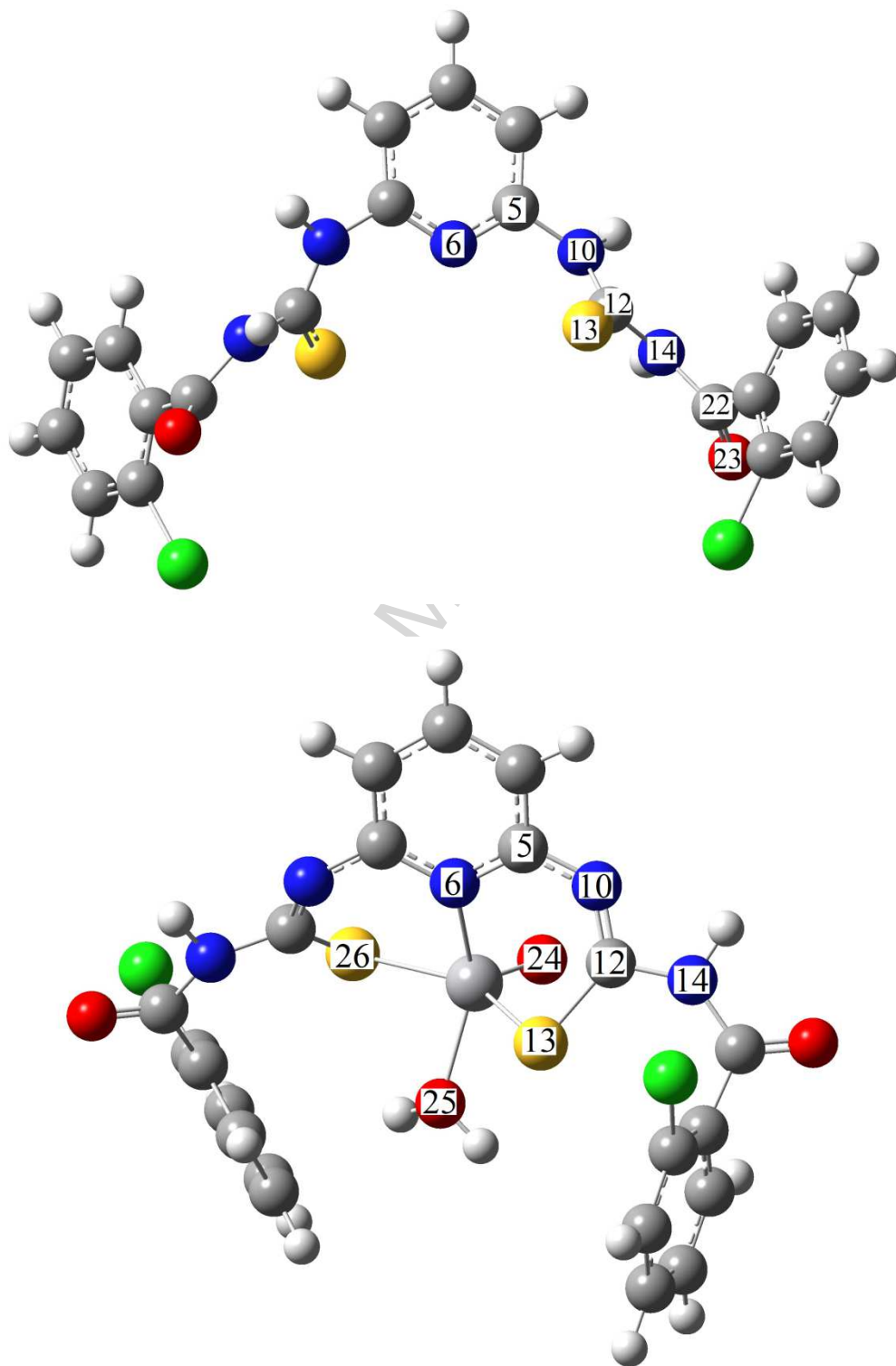
Fig 5. ORTEP representation of C4. Displacement ellipsoids are drawn at the 50% probability level and H atoms are shown as small spheres of arbitrary radii.

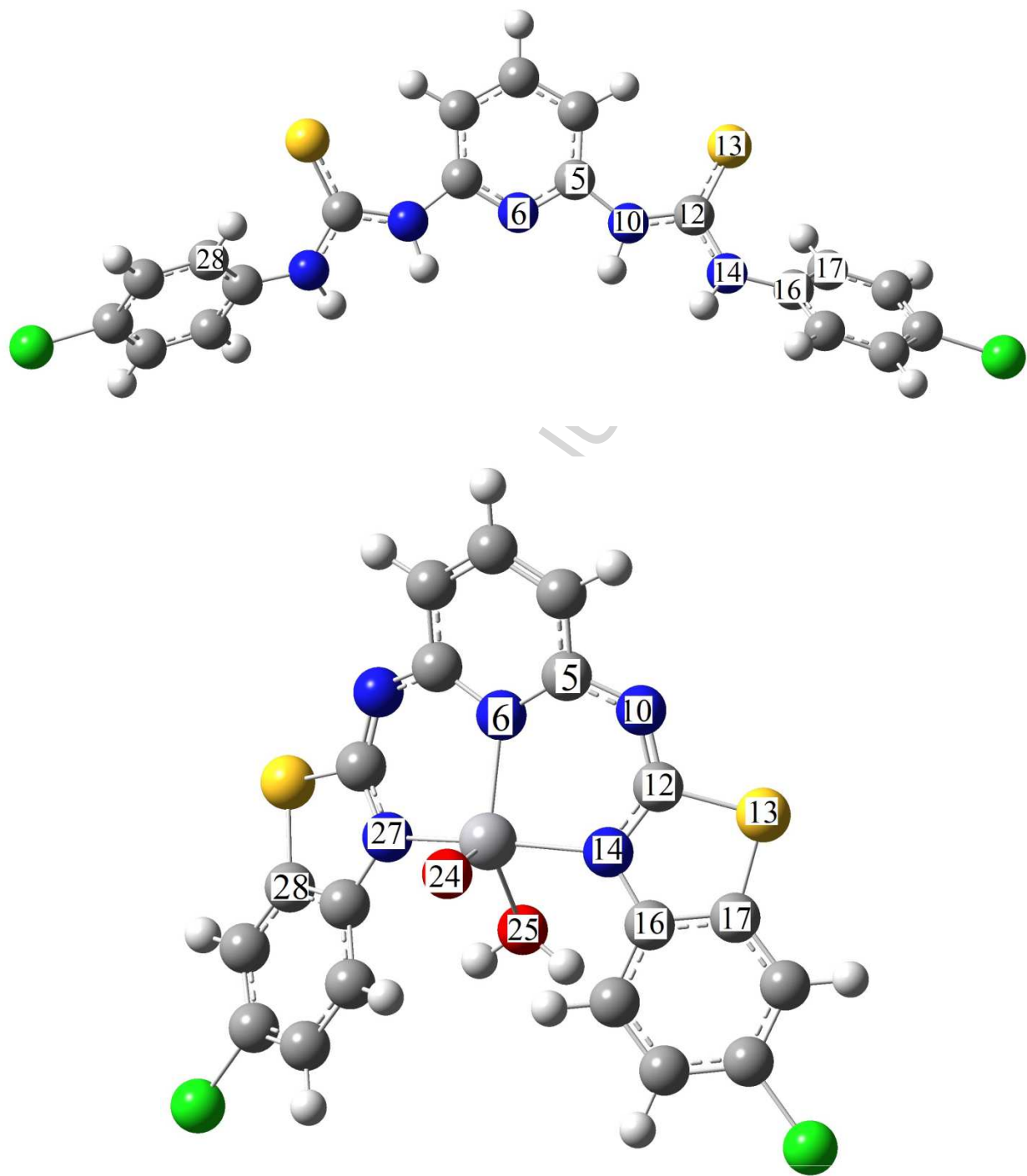
Fig. 6. The intermolecular hydrogen bonds between the biguanidium groups and the carboxylate groups of the dipic-OH, between the oxo groups and the water molecules, as well as between the carboxylate groups of dipic-OH and water molecules with donor. . .acceptor distance.

Fig. 7. The linear relations between the energies of LUMOs and the inhibition zones (a) for *P. aeruginosa* in L1, C1, C2 and C3 samples; (b) for *E. faecalis* in C1, C2 and C3 samples and (c) for *P. aeruginosa* in C1, C2 and C3 samples.

Fig. 8. The linear relations of the differences between the LUMO and HOMO energies and the inhibition zones (a) for *P. aeruginosa* in L2, L3, C1, C2, C3 and C4 samples; (b) for *E. faecalis* in L1, L2, L3, C1, C2 and C3 samples; (c) for *S. aureus* in L2, C1, C2 and C3 samples and (d) for *E. coli* in C1, C2 and C3 samples.

**Fig. 1.**

**Fig. 2.**

**Fig. 3.**

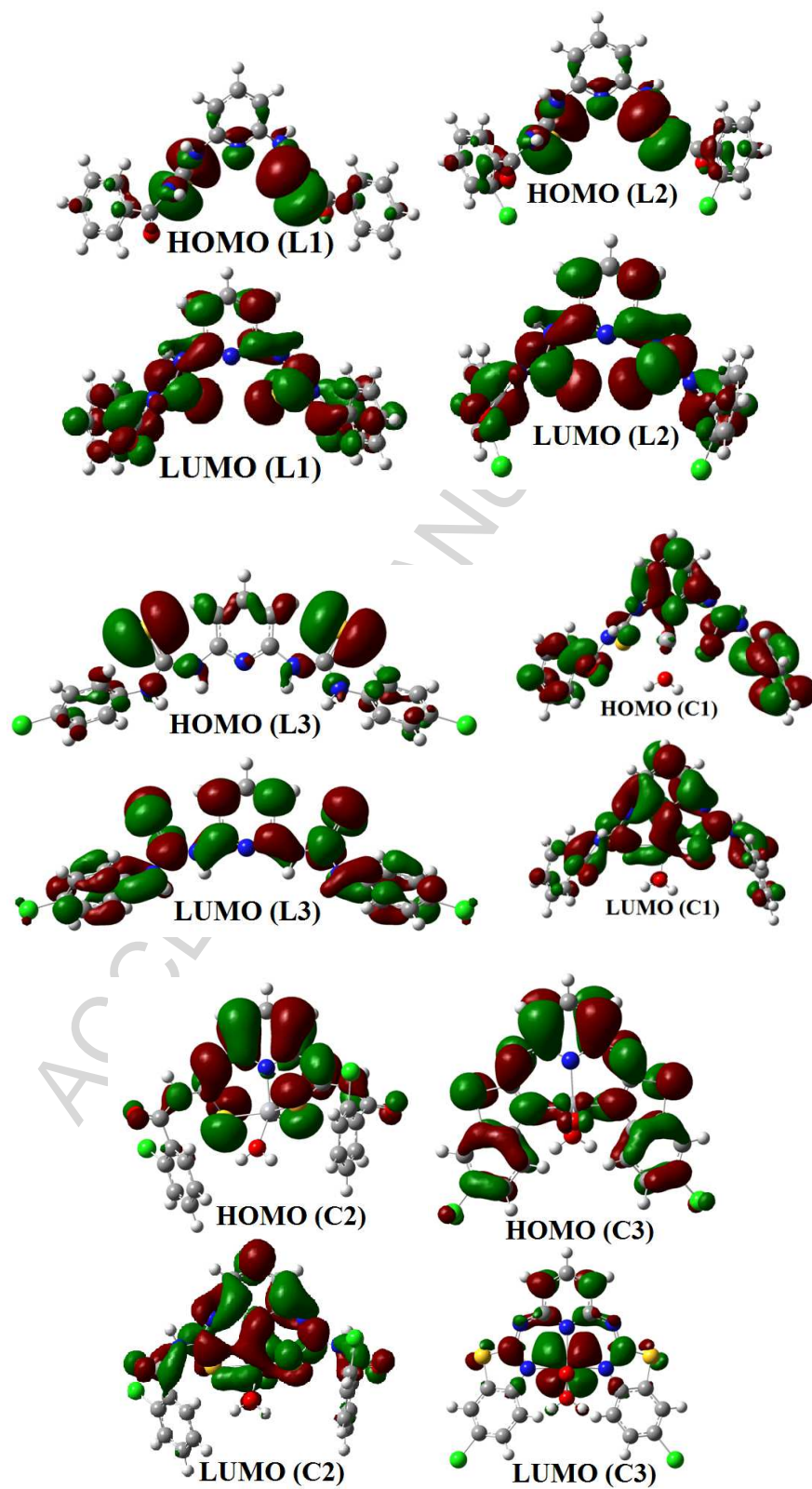


Fig. 4.

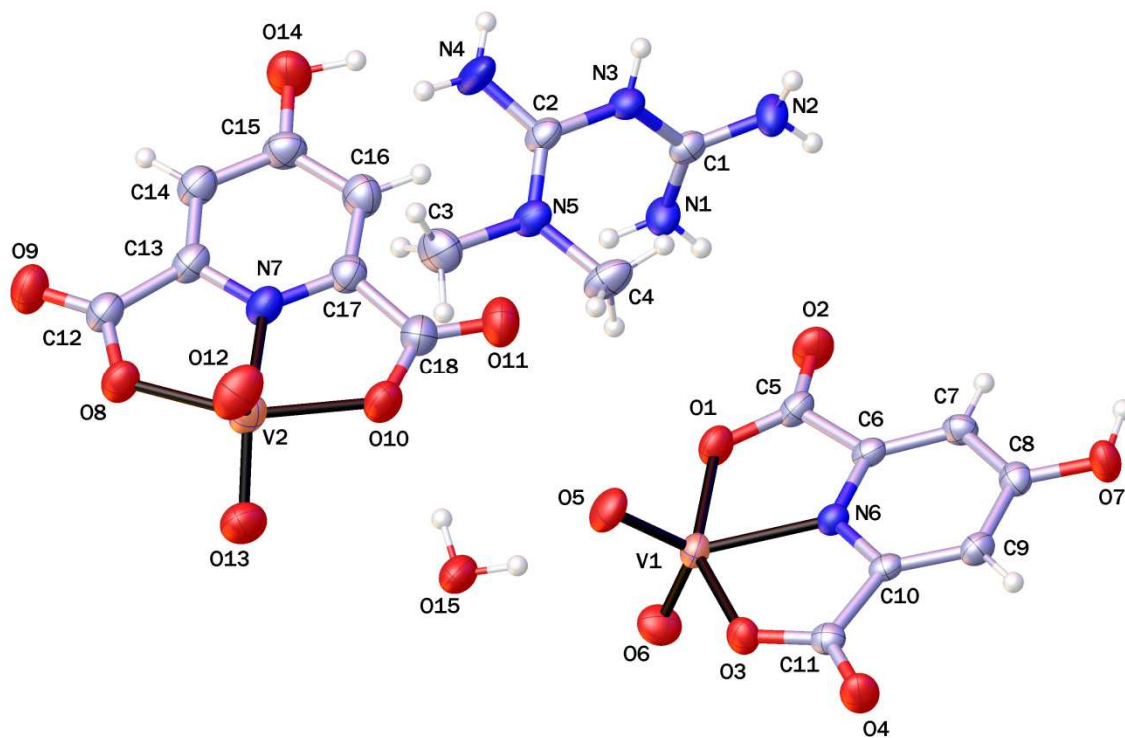


Fig 5.

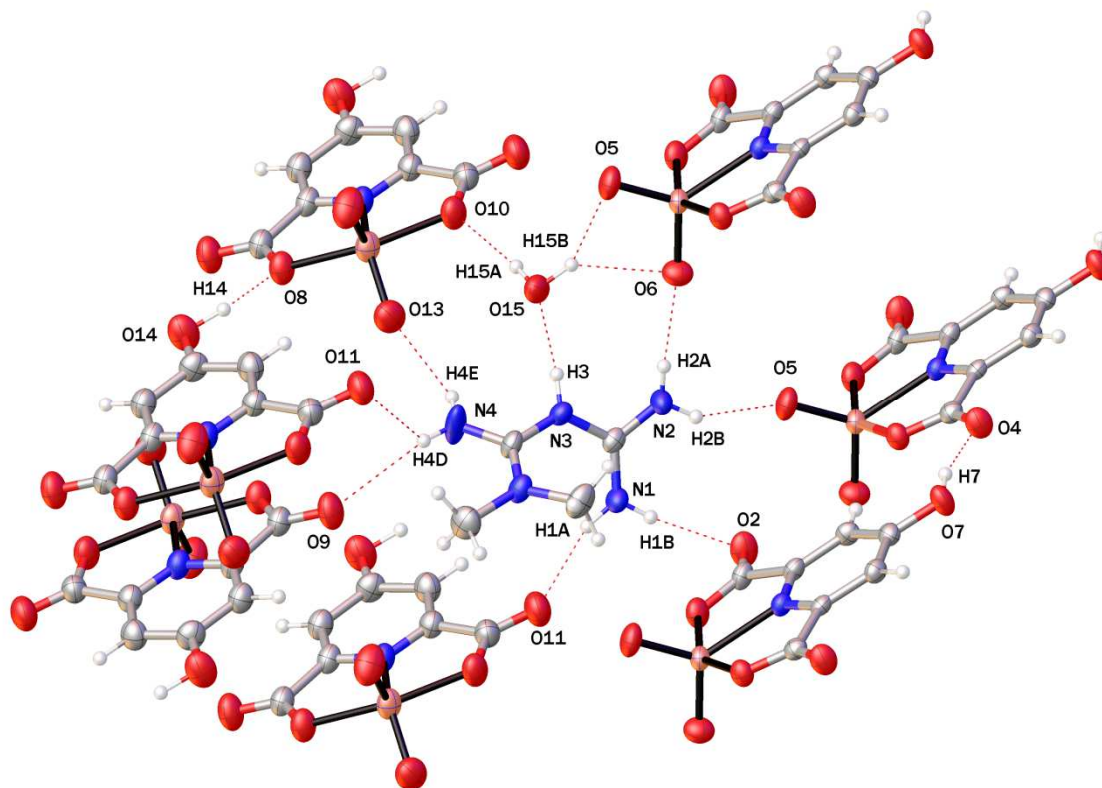
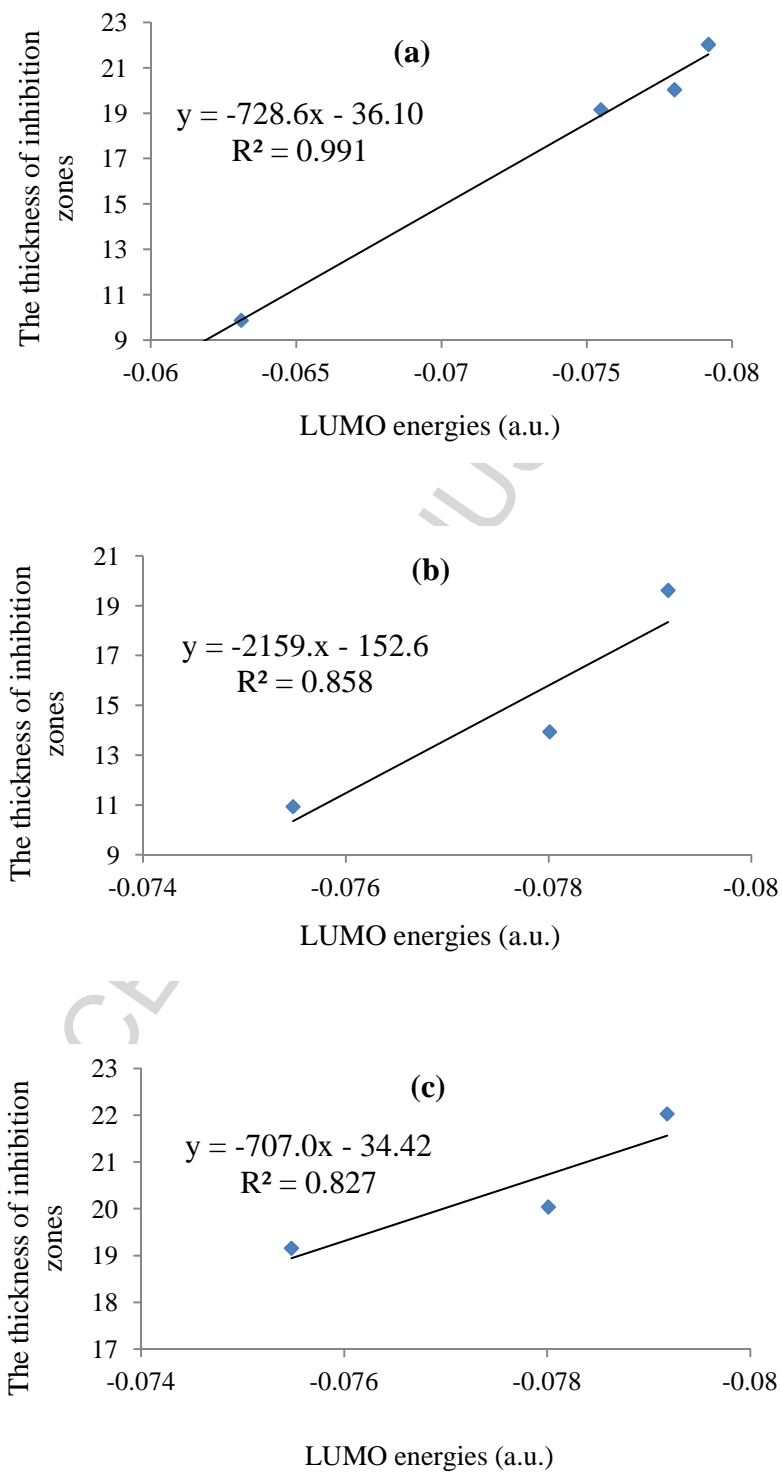


Fig. 6.

**Fig. 7.**

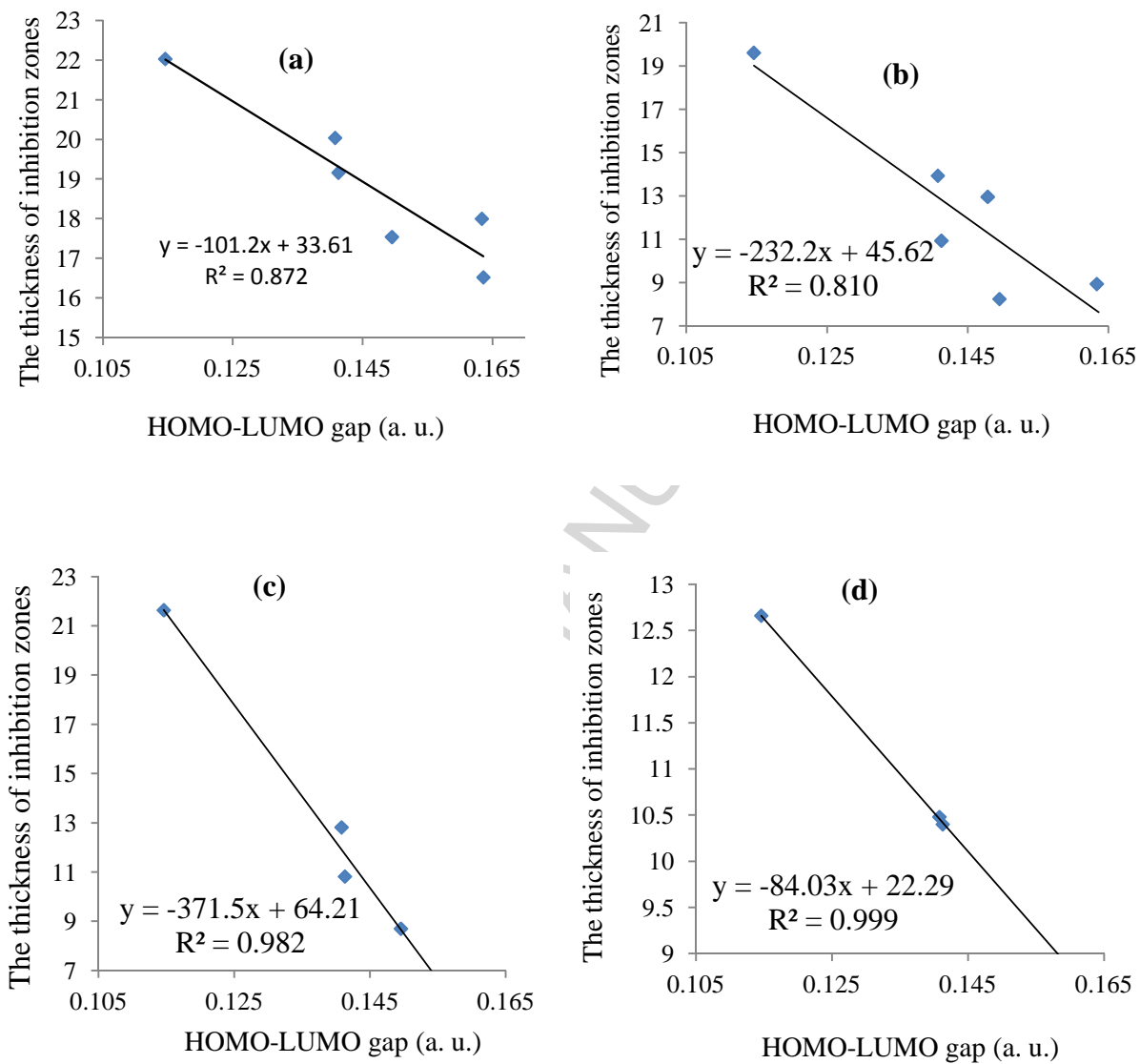


Fig. 8.

Table 1. Crystal data and structure refinement for complex C4

Empirical formula	$C_{18}H_{21}N_7O_{15}V_2$
Molecular weight	677.30
Temperature (K)	293(2)
Crystal system	Triclinic
Space group	$P\bar{1}$
a (Å)	6.7449(2)
b (Å)	8.0197(2)
c (Å)	23.0292(7)
α (°)	92.764(2)
β (°)	93.888(2)
γ (°)	95.540(2)
Volume (Å ³)	1235.14(6)
Z	2
D_{calc} (g cm ⁻³)	1.821
Absorption coefficient (mm ⁻¹)	0.849
$F(000)$	688
Crystal size (mm)	0.45 × 0.43 × 0.29
Theta range for data collection	2.66 to 25.00°
Index range	$-8 \leq h \leq 8$ $-9 \leq k \leq 9$ $-27 \leq l \leq 27$
Reflections collected	39455
$R(\text{int})$	0.0516
Final R indices [$I > 2\sigma(I)$]	$R_1 = 0.0440$, $wR_2 = 0.1088$
R indices (all data)	$R_1 = 0.0590$, $wR_2 = 0.1199$
Goodness-of-fit on F^2	1.059

Largest peak/hole [$e \text{ \AA}^{-3}$]-0.719/0.683

ACCEPTED MANUSCRIPT

Table 2. The selected structure parameters of DFT of thiourea ligands

	L1	L2	L3
<i>Bond Length (Å)</i>			
N6-C5	1.329	1.329	1.340
C5-N10	1.411	1.412	1.406
N10-C12	1.382	1.382	1.377
C12-S13	1.651	1.650	1.670
C12-N14	1.402	1.401	1.382
N14-C22	1.415	1.408	—
C22-O23	1.220	1.216	—
N14-C16	—	—	1.415
<i>Angle (°)</i>			
N6-C5-N10	117.45	117.34	110.91
C5-N10-C12	127.97	127.62	133.44
N10-C12-S13	125.66	125.63	125.89
N10-C12-N14	108.74	108.88	109.73
S13-C12-N14	125.60	125.49	124.38
C12-N14-C22	129.25	130.48	—
N14-C22-O23	117.66	118.18	—
C12-N14-C16	—	—	129.69
N14-C16-C17	—	—	123.04

Table 3. The selected structure parameters of DFT of thiourea complexes

	C1	C2	C3		C1	C2	C3
<i>Angle (°)</i>				<i>Bond Length (Å)</i>			
N6-C5-N10	123.94	123.01495	124.28	N6-C5	1.374	1.37408	1.393
C5-N10-C12	129.60	128.13778	126.66	C5-N10	1.374	1.37586	1.362
N10-C12-S13	127.22	126.8722	117.40	N10-C12	1.293	1.29162	1.292
N10-C12-N14	113.40	112.64934	130.09	C12-S13	1.763	1.75282	1.797
C12-S13-C17	—	—	89.87	C12-N14	1.391	1.40701	1.357
C12-N14-C16	—	—	112.37	V-S13	2.400	2.39585	—
C12-S13-V	99.49	98.16496	—	V-N14	—	—	2.060
C12-N14-V	—	—	121.76	V-N6	2.087	2.09171	2.096
N6-V-S13	92.22	91.02415	—	V-O24	1.563	1.56249	1.569
N6-V-N14	—	—	90.25	V-O25	2.105	2.10023	2.094
N6-V-O24	107.18	107.74616	116.65	S13-C17	—	—	1.756
N6-V-O25	145.84	143.94332	127.52	N14-C16	—	—	1.393
O24-V-O25	106.90	143.94332	115.83				
S13-V-O24	103.03	102.77995	—				
S26-V-O24	106.87	106.55816	—				
N14-V-O24	—	—	99.52				
N27-V-O24	—	—	99.52				
S13-V-S26	149.07	149.98935	—				
N14-V-N27	—	—	158.40				

Table 4. Some theoretically computed HOMO, LUMO energies, dipole moments and atom charges of thiourea ligands and complexes

<i>Charge</i>	L1	L2	L3	C1	C2	C3	C4
N6	-0.4429	-0.4411	-0.5458	-0.5658	-0.56497	-0.6197	—
N10	-0.6344	-0.6349	-0.6117	-0.5593	-0.54618	-0.5696	—
C12	0.2210	0.2217	0.2515	0.3151	0.29805	0.3177	—
S13	-0.0848	-0.0774	-0.1843	-0.1986	-0.16812	0.4122	—
N14	-0.6931	-0.6843	-0.6131	-0.6639	-0.65012	-0.6351	—
O23	-0.5653	-0.5458	—	-0.5696	-0.55282	—	—
E_{HOMO} (a.u.)	-0.21096	-0.21454	-0.21904	-0.21674	-0.21878	-0.19377	-0.12021
E_{LUMO} (a.u.)	-0.06311	-0.06502	-0.05569	-0.07548	-0.07801	-0.07918	0.0434
$\Delta E_{\text{L-H}}$	0.14785	0.14952	0.16335	0.14126	0.14077	0.11459	0.16361
μ (debye)	8.0194	10.6116	4.8643	2.2506	4.366	2.1629	—

Table 5. Selected bond lengths [\AA] and angles [deg] for
 $[\text{H}_2\text{Met}][\text{VO}_2(\text{dipic-OH})_2]\cdot\text{H}_2\text{O}$

V(1)-O(5)	1.614(2)	V(2)-O(13)	1.603(3)
V(1)-O(6)	1.617(3)	V(2)-O(12)	1.606(3)
V(1)-O(1)	1.977(3)	V(2)-O(10)	1.996(3)
V(1)-O(3)	1.990(2)	V(2)-O(8)	2.024(3)
V(1)-N(6)	2.072(3)	V(2)-N(7)	2.076(3)
O(5)-V(1)-O(6)	109.17(15)	O(13)-V(2)-O(12)	109.93(17)
O(5)-V(1)-O(1)	98.57(12)	O(13)-V(2)-O(10)	96.31(14)
O(6)-V(1)-O(1)	98.96(13)	O(12)-V(2)-O(10)	101.30(15)
O(5)-V(1)-O(3)	98.91(12)	O(13)-V(2)-O(8)	98.71(14)
O(6)-V(1)-O(3)	99.29(12)	O(12)-V(2)-O(8)	100.42(14)
O(1)-V(1)-O(3)	148.91(10)	O(10)-V(2)-O(8)	147.46(12)
O(5)-V(1)-N(6)	129.41(13)	O(13)-V(2)-N(7)	132.21(15)
O(6)-V(1)-N(6)	121.41(13)	O(12)-V(2)-N(7)	117.85(16)
O(1)-V(1)-N(6)	74.83(10)	O(10)-V(2)-N(7)	74.49(12)
O(3)-V(1)-N(6)	74.20(10)	O(9)-V(2)-N(2)	74.02(11)

Table 6. Hydrogen bond details, distances (Å) and angles (°)
for [H₂Met][VO₂(dipic-OH)]₂·H₂O.

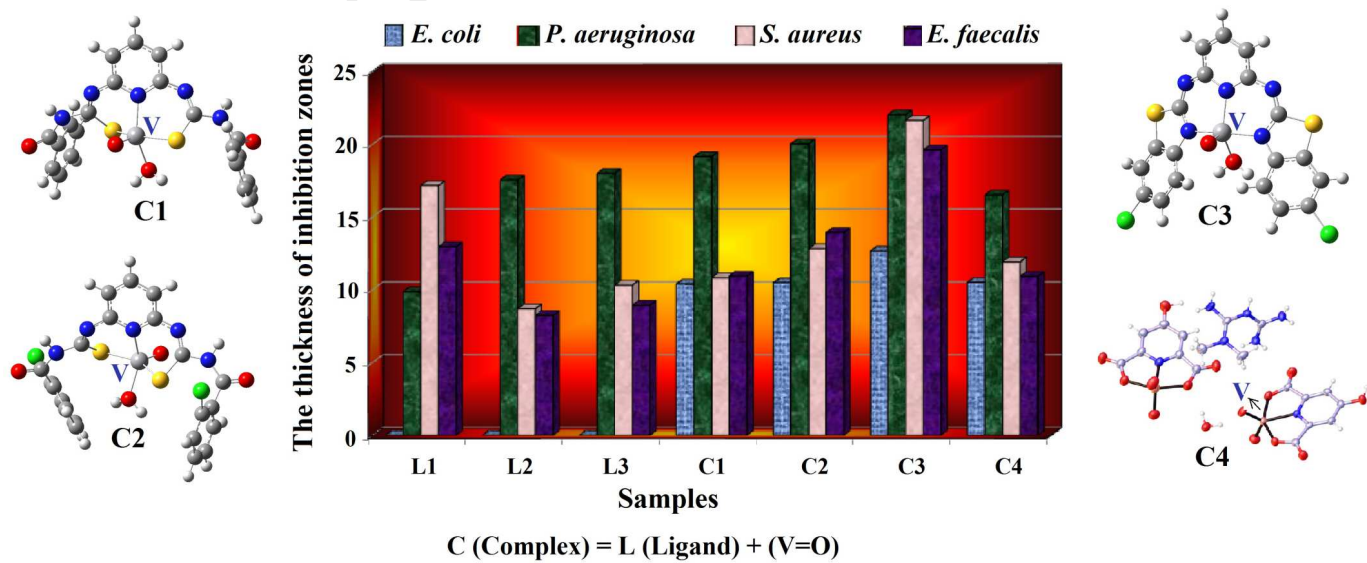
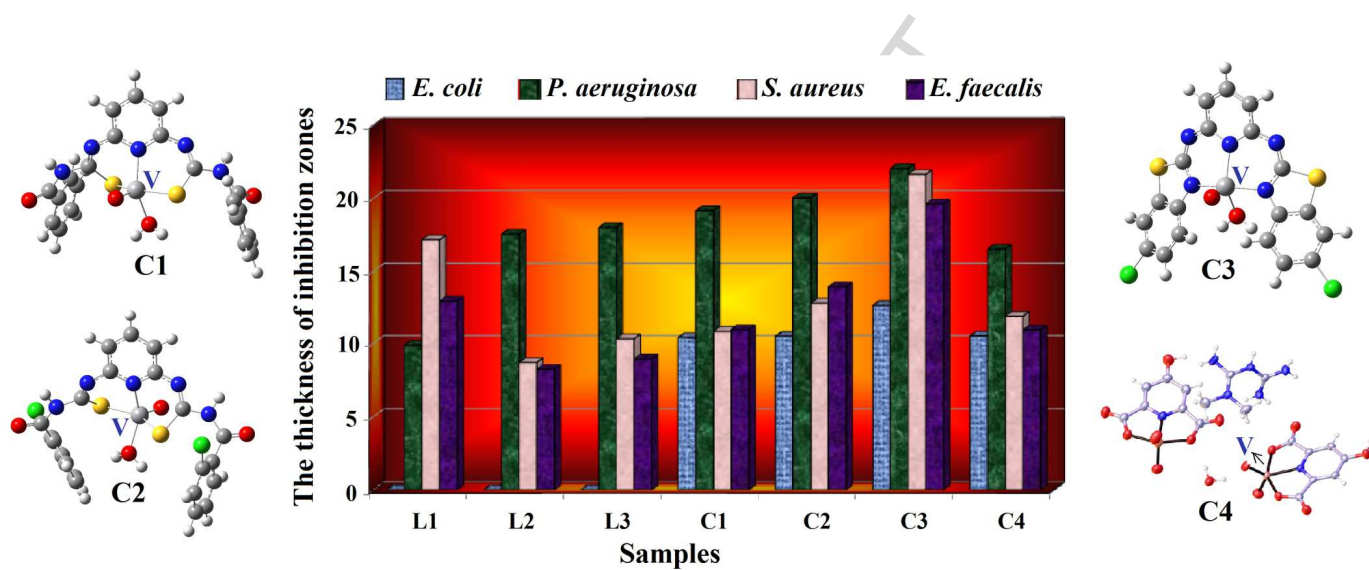
<i>D</i> -H... <i>A</i>	<i>D</i> -H	H... <i>A</i>	<i>D</i> ... <i>A</i>	<i>D</i> -H... <i>A</i>
N(1)-H(1A)...O(11)	0.85(3)	2.05(3)	2.869 (4)	162(4)
N(1)-H(1B)...O(2)	0.85(3)	2.20(3)	2.933 (4)	148(3)
N(2)-H(2A)...O(6) ⁱ	0.85(3)	2.04(3)	2.878 (4)	166(3)
N(2)-H(2B)...O(5) ⁱⁱ	0.85(3)	2.15(4)	2.914 (4)	150(4)
N(3)-H(3)...O(15) ⁱ	0.87(3)	1.86(3)	2.217 (4)	170(3)
N(4)-H(4D)...O(11) ⁱⁱⁱ	0.85(4)	2.56(5)	3.120 (6)	124(4)
N(4)-H(4D)...O(9) ^{iv}	0.85(4)	2.51(4)	3.224 (5)	143(4)
N(4)-H(4E)...O(13) ⁱ	0.85(4)	2.22(4)	2.909 (6)	138(4)
O(7)-H(7)...O(4) ⁱⁱ	0.93(3)	1.87(2)	2.760 (3)	161(4)
O(14)-H(14)...O(8) ⁱⁱ	0.99(5)	1.70(5)	2.648 (4)	158(4)
O(15)-H(15A)...O(10)	0.93(4)	1.91(4)	2.787 (4)	157(4)
O(15)-H(15B)...O(5)	0.93(5)	2.20(5)	3.028 (4)	148(6)
N(15)-H(15B)...O(6)	0.93(5)	2.27(5)	3.026 (4)	139(6)

Symmetry codes: (i) 1+x,1+y,z; (ii) x,1+y,z; (iii) 1+x,y,z; (iv) 2-x,1-y,1-z.

Table 7. The values of minimal inhibitory concentrations (MIC, $\mu\text{g/ml}$) and zones of inhibitions (ZI, diameter/mm) of the all compounds against the studied bacterial strains.

Samples	E. coli		P. aeruginosa		S. aureus		E. faecalis	
	MIC	ZI	MIC	ZI	MIC	ZI	MIC	ZI
L1	512	-	512	9.87	128	17.16	256	12.96
L2	512	-	512	17.54	512	8.70	512	8.24
L3	1024	-	512	18.00	1024	10.32	512	8.94
C1	512	10.40	64	19.16	256	10.82	512	10.94
C2	512	10.48	64	20.04	256	12.82	256	13.94
C3	256	12.66	128	22.03	64	21.64	256	19.62
C4	512	10.51	256	16.52	512	11.93	512	10.92
DMSO	-	-	-	-	-	-	-	-
AMK	-	-	-	-	-	18.50	-	18.50
GEN	-	23.72	-	23.72	-	-	-	-

Graphical abstract



Synopsis for the Graphical abstract**Graphical abstract**

Three new thiourea ligands, their oxo-vanadium(IV) complexes and oxo-vanadium(V) complex containing 4-hydroxy-2,6-pyridine dicarboxylic acid and metformin were synthesized. The antibacterial properties of all compounds were screened in vitro against standard bacterial strains.

Research highlights

- Three new thiourea ligands and their oxido-vanadium(IV) complexes have synthesized.
- The complexation with vanadium leads to increment in the biological activity of thiourea ligands.
- The LUMO and HOMO energies have some relationship with antibacterial activities in these compounds.